Journal of Pharmaceutical Sciences 107 (2018) 807-813

Contents lists available at ScienceDirect

Journal of Pharmaceutical Sciences

journal homepage: www.jpharmsci.org

Drug Discovery—Development Interface

Rapid, Room Temperature Nanoparticle Drying and Low-Energy Reconstitution via Electrospinning

Shani L. Levit, Ratib M. Stwodah, Christina Tang*

Department of Chemical and Life Science Engineering, Virginia Commonwealth University, 601 West Main Street, Box 843028, Richmond, Virginia 23284

ARTICLE INFO

Article history:
Received 8 August 2017
Revised 29 September 2017
Accepted 17 October 2017
Available online 26 October 2017

Keywords:
nanoparticles
drying
polymers
stabilization
nanotechnology

ABSTRACT

Nanoparticle formulations offer advantages over free drugs; however, stability of the nanoparticle dispersions is a significant obstacle, and drying is often required for long-term size stability. The main limitation of current drying methods is particle aggregation upon reconstitution which can be overcome with sonication (impractical in a clinical setting) or large amounts of cryoprotectants (result in hypertonic dispersions). Therefore, new approaches to nanoparticle drying are necessary. We demonstrate conversion of nanoparticle dispersions to a dry, thermostable form via electrospinning. As a proof-of-concept, polyethylene glycol stabilized nanoparticles and polyvinyl alcohol were blended and electrospun into ~300 nm fibers. Following electrospinning, nanoparticles were stored for at least 7 months and redispersed with low osmolarity to their original size without sonication. The nanoparticles redisperse to their original size when the fiber diameter and nanoparticle diameter are comparable (nanoparticle:nanofiber ratio ~1). Nanoparticles with liquid cores and larger particles better maintained their size when compared to nanoparticles with solid cores and smaller particles, respectively. Storing the nanoparticles within nanofibers appears to prevent Ostwald ripening improving thermostability. Overall, this novel approach enables rapid, continuous drying of nanoparticles at room temperature to facilitate long-term nanoparticle storage. Improved nanoparticle drying techniques will enhance clinical translation of nanomedicines.

Introduction

Nanoparticle (NP) drug formulations offer advantages over free-drug formulations such as increased bioavailability and intracellular accumulation with relatively low toxicity.[1-3] However, stability of the NP dispersions is a considerable obstacle.[4] Often, cold chain storage is required to prevent Ostwald ripening. The requirement of cold chain storage is challenging for clinical applications.[5] Often, to achieve stable formulations with long shelf-lives, complete drying of the sample is required.[6,7] However, maintaining NP size during drying remains a significant challenge.

Three techniques commonly used for drying drug-loaded NPs are freeze drying, spray drying, and more recently spray freeze drying.[7-13] Freeze drying is a 3-step process in which the solvent is removed with an initial freezing step followed by sublimation and desorption.[14] Spray drying is a continuous process in which the NP dispersion is cast into droplets that are rapidly dried with a hot gas.[15-17] Spray freeze drying is an integration of the 2 methods in which the solution is cast into droplets that are immediately frozen followed by sublimation of the remaining liquid.[18] While some particle formulations have been successfully dried,[17,19] the main limitation of current drying methods is particle aggregation after drying and reconstitution so the nanometer particle size, which is vital for therapeutic efficacy,[20,21] cannot be maintained.[14,22] For example, after freeze drying, β-carotene- and paclitaxel-loaded NPs made by flash nanoprecipitation (FNP) method, redispersions resulted in at least a 2.25-fold increase in particle size even with sonication, a process which is considered impractical in a clinical setting.[6,23] Freeze-dried vitamin E (VE) NPs stabilized with polystyrene-b-polyethylene glycol (PS-b-PEG) that were made via FNP exhibited a 3-fold increase in size after reconstitution with sonication.[6] Therefore, new approaches to NP drying that maintain NP size after reconstitution are necessary.

Cryoprotectants or excipients, such as glucose, sucrose, and trehalose, and so forth, can prevent aggregation.[9,24] However, significant amounts of protectant/excipient are generally required.[9,19,25] For example, spray freeze drying polycaprolactone NPs required concentrations of 70 wt.% mannitol to achieve a final

This article contains supplementary material available from the authors by request or via the Internet at https://doi.org/10.1016/j.xphs.2017.10.026.

* *Correspondence to:* Christina Tang (Telephone: +1 (804)-827-1917; Fax: +1 (804)-827-3026).
E-mail address: ctang2@vcu.edu (C. Tang).

https://doi.org/10.1016/j.xphs.2017.10.026
0022-3549/

NP size to initial NP size (S_f/S_i) ratio of 1.5.[19] When freeze drying drug-loaded NPs using trehalose as a cryoprotectant, a mass ratio of 5:1 trehalose: NPs was required for redispersion.[23] The large amount of protectant is problematic for parenteral administration because the osmolarity of the protectant can result in a hypertonic formulation (> 240 mOsm/kg).[6]

We present electrospinning NPs blended with a water-soluble polymer as an alternative to traditional drying techniques to rapidly convert NP dispersions to a dry form that can be stored at room temperature. In electrospinning, the polymer blend is extruded at a constant rate and when the force due to an applied electric field overcomes surface tension, a liquid jet forms. As the liquid jet travels to a grounded collector, it is whipped and stretched and the solvent rapidly evaporates creating a solid fiber.[26-30] The fiber is deposited as nonwoven. Electrospinning the blend of NPs and a water-soluble polymer, the NPs are encapsulated within the resulting polymer fibers. The nonwoven material can be stored at room temperature, and the fibers are dissolved in aqueous media to reconstitute the NPs.

The use of polymers as excipients are a promising alternative to saccharides because they can be added at high mass ratios relative to the NPs without creating hypertonic formulations. Polymers, such as polyvinyl alcohol (PVA), used as excipients in traditional drying techniques, spray drying, and spray freeze drying[31] have been considered. Approaches using polymers in techniques such as electrospinning and electroblowing have been employed for preserving amorphous formulations of small molecules.[32] However, the applicability of such techniques for converting NPs to a dry, stable form has yet to be demonstrated.

In this work, we demonstrate electrospinning as a rapid, room temperature method to convert NP dispersions to a dry, thermostable form that can be redispersed to the original NP size without sonication. We use NP formulations sterically stabilized with polyethylene glycol (PEG) as a model system because PEG coatings increase circulation time and delay clearance by the mononuclear phagocytic system.[33-36] Such particles can be fabricated using FNP, a rapid and scalable method. In FNP, PEGylated block copolymers direct NP self-assembly during rapid mixing of the hydrophobic drug and block copolymer dissolved in an organic stream with a miscible antisolvent stream. Owing to the rapid mixing, the NPs are kinetically trapped with high core material loading capacities, narrow size distribution, and tunable size.[37] Blends of the PEGylated FNP particles with PVA were electrospun to convert the NPs into a stable, dry form. PVA was selected as a starting point for these experiments because it is often included in freeze-dried formulations.[14,31] The NPs were reconstituted to their original size without sonication. The effect of fiber processing on final NP size was explored. Specifically, we examined the effect of NP composition, NP size, and NP to fiber diameter ratio.

Materials and Methods

Materials

NPs were formulated with amphiphilic block copolymer, PS-b-PEG (1600-b-5000 g/mol) obtained from Polymer Source (Montreal, Canada). PS-b-PEG was dissolved in tetrahydrofuran (THF) (~40°C) and precipitated into diethyl ether and dried under vacuum. For the NP core material, α-tocopherol (Vitamin E, VE; Sigma-Aldrich, St. Louis, MO) and PS with molecular weight (MW) = 800-5000 Da (Polyscience, Inc., Warrington, PA) were used. THF was used as the solvent (HPLC grade; Fisher Scientific, Pittsburgh, PA). The electrospinning polymer was PVA with MW = 205,000 Da (Mowiol 40-88; Sigma-Aldrich). All other reagents were used as received.

Nanoparticle Preparation

NPs were prepared via FNP with a hand-operated confined impinging jet mixer with dilution.[37] In FNP, the hydrophobic core material is initially molecularly dissolved in an organic solvent with the amphiphilic block copolymer stabilizer and is rapidly mixed with a miscible, nonsolvent for the hydrophobic core. This rapid mixing with the nonsolvent decreases the solvent quality for the core material and hydrophobic block of the amphiphilic block copolymer that is, decreases the solubility of the core material and hydrophobic block of the stabilizer which induces simultaneous precipitation of the core material and micellization of the block copolymer. Adsorption of hydrophobic block on the precipitating core material arrests NP growth and the hydrophilic block sterically stabilizes the NP.[38] In a typical experiment, PS-b-PEG was dissolved in THF with core material (VE or PS) at a total solids concentration ~30 mg/mL. Typically, 0.5 mL of the organic stream was rapidly mixed with an equal amount of water (miscible nonsolvent for the hydrophobic core material) and immediately diluted with 4 mL of water to maintain a THF:water ratio of 1:9 by volume. The ratio of the block copolymer to core material was varied to tune the size of the NPs based on pervious studies.[37] Following mixing, the organic solvent was removed by dialysis, using regenerated cellulose tubing with a MW cutoff of 6-8 kDa (Spectra/Por; Spectrum Laboratories, Houston, TX), against a 100-fold volume of water for 24 h with 4 changes of the bath. NP size before and after dialysis were measured using dynamic light scattering (DLS).

Initial Nanoparticle Characterization

The mean particle size and distribution was determined by DLS using a Malvern Zetasizer ZS (Malvern Instruments Ltd., Malvern, UK) with a backscatter detection angle of 173°. Initial particle size distributions are reported using the normal resolution model intensity weighted distribution (average of 4 measurements). For the initial NP size, particle uniformity was defined as size distribution with a single Gaussian peak. The polydispersity index is a measure of the breadth of the particle distribution defined from the moments of the cumulant fit of the autocorrelation function calculated by the instrument software as previously described.[37]

Electrospinning

For electrospinning, aqueous solutions of PVA were prepared by dissolving 9.5 wt.% PVA in water. The PVA was stirred at 60°C overnight until the solution was macroscopically homogeneous and stored at 4°C. The NPs in water (after dialysis) and dissolved PVA were combined in various proportions and stirred for several minutes at room temperature until macroscopically homogenous. The final PVA concentration for electrospinning was 7 wt.% based on previous studies.[39] The NP loading (mass of NPs per mass of PVA) was systematically varied.

The blend of polymer and NPs was electrospun using a conventional setup.[39] Briefly, the polymer-NP blend was pumped (New Era Pump System, Inc., Farmingdale, NY) through a 22-gauge (inner diameter = 0.508 mm) stainless steel needle (Jensen Global, Santa Barbara, CA) at a constant rate while applying a constant voltage (Matsusada High Precision Inc., Shiga, Japan). Typical, process parameters were tip-to-collector distance of 15 cm, applied voltage of 13-15 kV, and flow rate of 0.5 mL/h. Blends were electrospun for 20 min so the resulting mat was thick enough to easily remove from the foil. Each solution was electrospun in triplicate and stored at ambient conditions.

Table 1
Characteristics of NP-Loaded Electrospun Fibers

Core Material	Initial NP Diameter (nm)	NP Loading wt.%	Nanofiber Diameter (nm)
VE	95 ± 4	0.8	365 ± 36
	118 ± 5	0.8	249 ± 32
	129 ± 2	0.8	326 ± 34
	144 ± 9	0.8	322 ± 56
	174 ± 2	0.8	291 ± 37
		1.7	303 ± 34
		3.2	292 ± 47
PS	112 ± 5	0.8	354 ± 31
	192 ± 14	0.8	390 ± 37

Nanofiber Characterization

The fiber samples were sputter-coated (POLARON E5400 SEM Coating system) with gold (~10 nm) or gold:palladium target 60:40 and analyzed with scanning electron microscopy (SEM) (JEOL LV-5610; JOEL, Peabody, MA) at an accelerating voltage of 20 kV. Images were taken at a magnification of 10,000× with a working distance of 10 mm. The average fiber diameter and standard deviation were determined by measuring the diameter of at least 75 fibers from 4 to 5 fields of view using ImageJ software.

Nanoparticle Reconstitution

The NPs were reconstituted by dissolving the resulting nanofibers (NFs) (after being removed from the foil and weighed) in deionized (DI) water. Mass of fibers to volume of DI water ratio was held constant at 0.4 mg fiber per mL of DI water. The redispersions were hand mixed for ~10 min with brief, intermittent vortexing until there were no visible aggregates. The reconstituted samples were syringe filtered (Whatman 0.45 μm nylon filter) and measured on DLS. The time between reconstitution and syringe filtering was varied and no significant effect of delay time was observed. This fiber to water ratio selected so that the dissolved polymer and NP sizes could be resolved using DLS to determine the NP size upon reconstitution post electrospinning. The NP size and polydispersity index were obtained using the Multiple Narrow Modes algorithm based on non-negative least squares fit using Zetasizer software as has been previously reported.[40,41] Since the resolution of DLS is inherently limited to a factor of 3,[42] only samples with a NP intensity peak size (nm)/PVA intensity peak size (nm) >3 are reported.

Results

Proof of Concept

PEG-stabilized NPs loaded with VE or PS homopolymer were fabricated with FNP. The size of the NPs was tuned by varying the ratio of core material to block copolymer stabilizer in the formulation.[37] The initial VE-loaded NPs were between 95 and 175 nm and PS-loaded NPs were between 110 and 190 nm (Table 1).

To demonstrate proof-of-concept of drying NPs via electrospinning, aqueous blends of NPs and a water-soluble polymer, PVA, were used as a model system. PVA was selected because its electrospinning has been well characterized.[39,43] PVA was used at concentration of 7 wt.% because there is sufficient molecular entanglement to facilitate fiber formation.[39,43,44] At 7 wt.% PVA and NP loading up to 3.2 wt.%, the PVA-NP blend solutions were electrospun to produce uniform fibers with no evidence of beading (Fig. 1). Since the fiber diameters were larger than the NPs, the NPs appear encapsulated within smooth PVA fibers. The fiber diameter and fiber size distribution (relative standard deviation) with and without VE or PS NPs were comparable (Fig. 1). Therefore, at the NP loadings used, the presence of the NPs did not significantly affect the PVA entanglement required for fiber formation. This result is comparable to other PVA-blend systems.[43] Thus, these results demonstrate that NPs can be converted into a dry form, that is, encapsulated within polymer fibers, by electrospinning a blend with a spinnable polymer.

Nanoparticle Reconstitution

For NP reconstitution, water was added to the PVA fibers followed by hand mixing. The polymer fibers start to dissolve immediately after the addition of water and appear completely dissolved within 5 min of hand mixing (Fig. 2). These results show that the NPs can be rapidly reconstituted using hand mixing (low-energy mixing). NPs reconstituted with hand mixing retain their initial size (S_f/S_i = 1.0-1.2) (Supplementary Data, Table C). Notably, previous results freeze drying (without excipient) similar particles

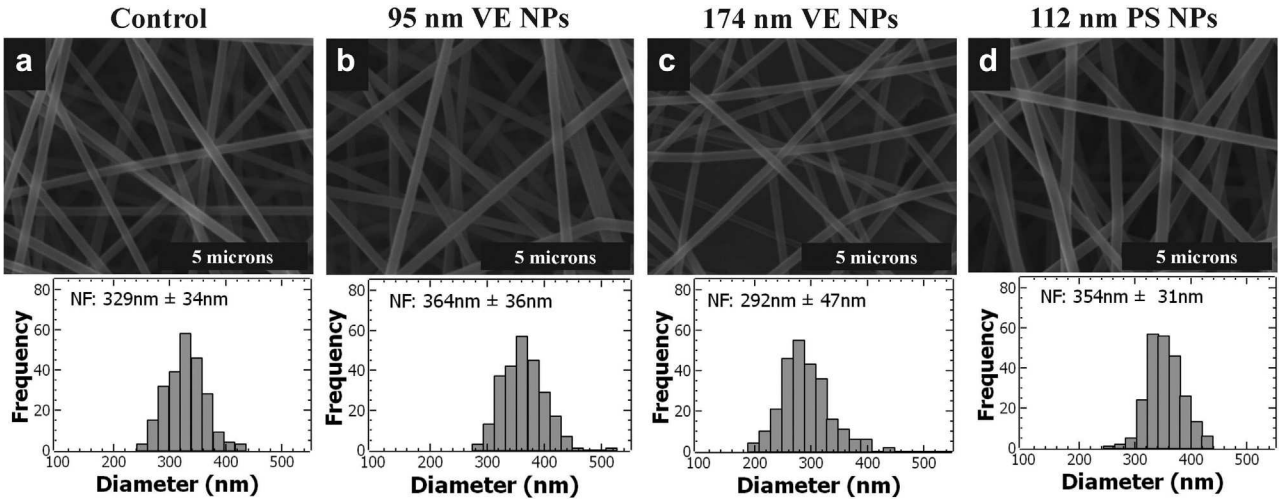

Figure 1. SEM images of electrospun PVA fibers loaded with NPs. (a) PVA only fibers with an average nanofiber (NF) diameter of 329 ± 34 nm, (b) PVA fibers with 95 nm VE NPs at 0.8 wt.% with an average NF diameter of 364 ± 36 nm, (c) PVA fibers with 3.2 wt.% loading of 174 nm VE NPs with an average diameter of 292 ± 47 nm, and (d) PVA fibers with 0.8 wt.% loading of 112 nm PS NPs and NF diameter of 354 ± 31 nm. All samples electrospun to form continuous, uniform fibers.

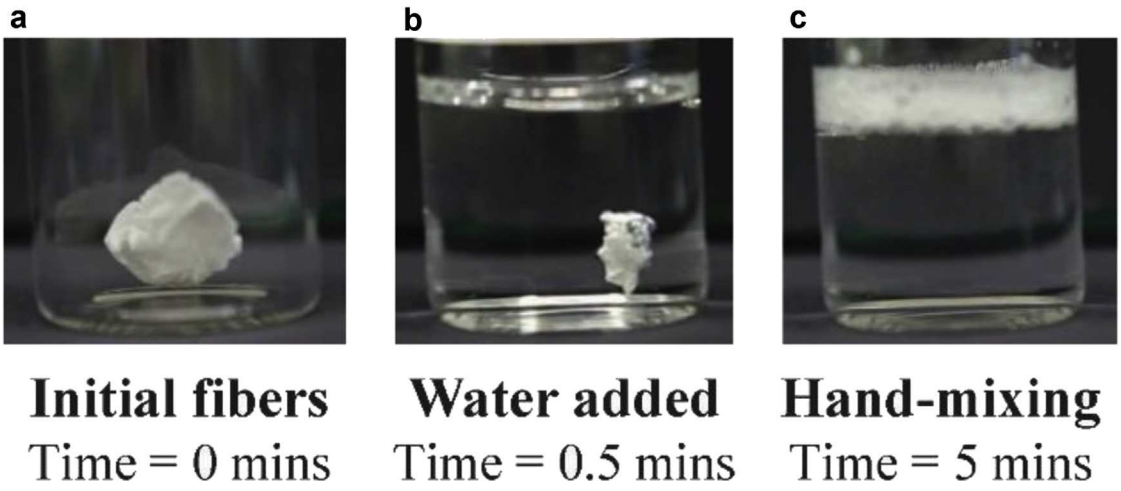

Figure 2. Rapid NP reconstitution using low-energy mixing. (a) Initial NP-loaded fibers (b) immediate dissolution of PVA fibers upon addition of DI water, and (c) visible confirmation of NP reconstitution within 5 min of hand mixing.

stabilized by PS-b-PEG did not retain their size as well. Sonication was required to obtain a S_f/S_i of 2.9[6]. Using PS-b-PEG-stabilized NPs as a model system suggests that drying NPs via electrospinning with PVA is a promising approach for converting NPs to a dry form while maintaining particle size.

The reconstitution of the NPs was examined by dissolving the fibers in phosphate buffer solution (PBS) and compared with water. All samples have 15%-16% change in size and a S_f/S_i of 1.1-1.2 (Supplementary Data, Table A). Thus, the buffer does not appear to alter the reconstitution of the NPs compared to dissolution in water. NPs can be reconstituted in PBS or water for potential clinical applications. Since the results were comparable when reconstituting in water or buffer, water was used in further experiments.

The osmolarity of the dispersion upon reconstitution is an important consideration in intravenous formulations. The PVA in the reconstituted solution of NPs has an approximate osmolarity of 0.002 mOsM. For comparison, the osmolarity of saline solution and PBS are 300 and 150 mOsM, respectively. Therefore, the polymer has a negligible contribution to the osmolarity of the final formulation when reconstituting in saline or buffer.

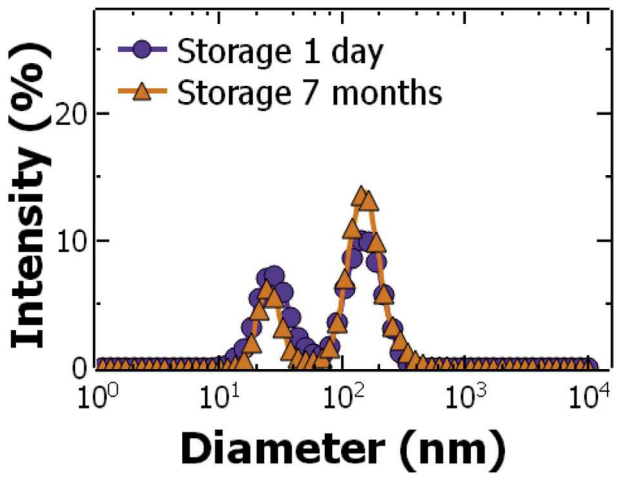

Figure 3. Particle size distribution measured by dynamic light scattering of 118 nm VE NPs reconstituted within 1 day of drying and after 7 months of storage at ambient conditions. The peak at ~30 nm is attributed to the dissolved polymer in the solution and the peak at ~160 nm is attributed to the reconstituted NPs. The NP size is comparable upon reconstitution after 1 day and 7 months of storage at ambient conditions.

Nanoparticle Storage

The shelf-life of the dry NPs in NFs at ambient temperature was examined using 120 nm VE NPs at a loading of 0.8 wt.%. The fiber sample was stored for 7 months at ambient conditions and then reconstituted. The NPs reconstituted from fibers after 1 day and after 7 months were comparable (Fig. 3). Notably, for the original NP dispersion stored at 4°C for 7 months, there was a 54% increase in diameter likely due to Ostwald ripening[20] (Table 2). These results suggest that converting the NP dispersion to a dry form, that is, encapsulated within the polymer fibers, prevents Ostwald ripening. Therefore, NP storage in NFs improves the size stability of NPs enabling storage of the NP formulations at room temperature and avoiding the need for cold chain storage.

Effect of Particle Properties

Nanoparticle Composition

Building on the results demonstrating proof-of-concept, we further probed the effect of fiber processing and particle properties on redispersed NP size. First, we investigated the effect of the composition of NP core by comparing VE- and PS-loaded NPs. The melting point of VE is 3°C which is below the working temperature of NP processing; therefore, VE core is expected to be in liquid phase. PS has a glass transition temperature of 100°C,[45] which is above the working temperature; therefore, the PS core is expected to behave as a solid. NPs of similar size were compared: the VE NPs had an initial diameter of 118 ± 5 nm and the PS NPs had an initial diameter of 112 ± 5 nm (Table 1). The fiber diameter was ~300 nm so the initial NP to NF diameter ratio (NP:NF) was 0.47 for both samples.

Using the Multiple Narrow Modes algorithm, the DLS results of the reconstituted NPs showed a bimodal distribution (Fig. 4). We

Table 2
Comparing Size Stability of NPs After Storage for 7 Months

Sample	Storage Temperature	Change in Size (%)
NPs in solution	4°C	54
Dried NPs	~23°C	4

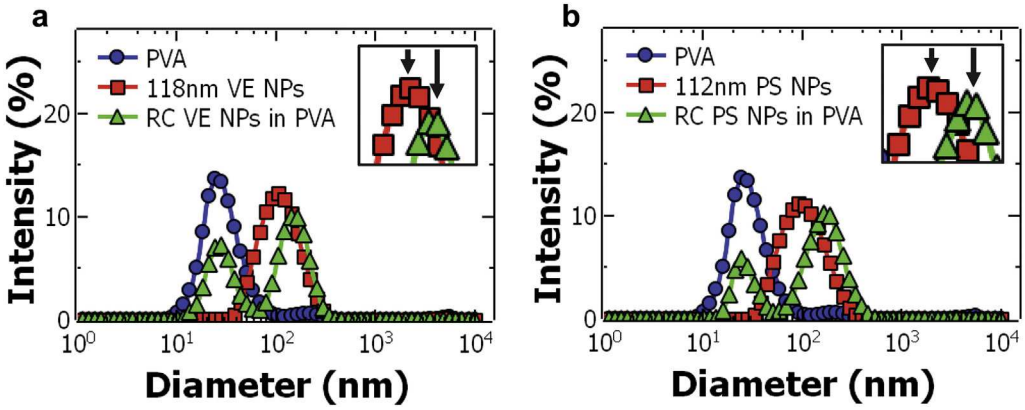

Figure 4. Particle size distribution measured by dynamic light scattering of the initial NPs, PVA control, and reconstituted (RC) NPs for (a) VE NP and (b) PS NPs. The NP peak shifts to the right indicative of an increase in particle size relative to initial NPs upon reconstitution.

attribute the peak at ~30 nm to the dissolved PVA and the second peak to the reconstituted NPs. The reconstituted NP size was taken as the NP peak intensity. For both VE and PS NPs, there was an increase in NP diameter upon reconstitution in water. When compared to the initial NP size, the final size to initial size (S_f/S_i) was 1.3 for the liquid core NPs and 1.7 for the solid core NPs (Table 3).

Interestingly, the increase in NP diameter in PS NPs was almost 2-fold greater than the VE NPs (i.e., 77 nm for PS NPs compared to 41 nm for VE NPs) (Table 3). This result suggests that NPs with a liquid core are more resistant to changes in size during fiber processing. Similar results have been observed with lyophilization[23] and were attributed to the ability of a NP with a liquid core to deform much more than a NP with a solid core. Since the liquid core particles deform, the forces experienced during drying are distributed over a larger area. In contrast, solid core particles that do not deform experience higher stresses (same force over a smaller area) which may cause aggregation.[23] In this method of drying, fiber formation involves uniaxial elongation of a viscous liquid jet,[46] as the solvent evaporates there is a transition from a liquid jet to a solid fiber, followed by stretching and thinning of the solid fiber. Since the diameter of the liquid jet is typically on the order of millimeters and much larger than the NP, we posit the shear forces have minimal influence on the NP deformation. As the jet is elongated and the solvent evaporates, it transitions from a liquid jet to a solid fiber (micron to nanometer diameter) resulting in high elongational stresses.[47] The elongational force as the fiber thins can cause the NPs to rotate and deform along the axis of shear stress.[48,49] The liquid core particles are expected to deform during fiber formation and redisperse into spheres close to the original size upon reconstitution. In contrast, the solid core particles may undergo some degree of aggregation during fiber formation and subsequent redispersion.

Effect of Nanoparticle Size

Next, we varied the initial size of the NPs at comparable NP:NF ratios. For VE NPs, the size of the NPs varied from 118 to 144 nm and the NP:NF ratio was ~0.5, that is, the NP diameter was approximately half of the final NF diameter. For PS NPs, the NP size varied from 112 to 192 nm and the NP:NF ratio was ~0.5. In both cases, the larger NPs better maintained their size upon electrospinning and redispersion compared to the smaller particles. For PS NPs, when the NP size increased from 112 to 192 nm, the change in NP size after reconstitution decreased from 69% to 16% resulting in a decrease in S_f/S_i from 1.7 to 1.2 (Table 3). A similar trend was observed with VE NPs. The change in VE NP size after reconstitution decreased from 35% to 17% resulting in a S_f/S_i from 1.3 to 1.2. This result may be because larger particles have larger surface area to distribute the forces the NPs are subjected to during fiber formation which reduces potential aggregation.

Effect of Nanoparticle Size Relative to Nanofiber Size

Based on these results, we investigated the effect of fiber size relative to the particle using VE NPs. The size of the VE NPs was varied between 95 and 175 nm (Table 1). When electrospun, the resulting fiber diameter was comparable and we examined the ratio of the NP diameter to NF diameter (NP:NF diameter). For NPs ~95 nm and fiber diameter ~300 nm (NP:NF ratio 0.26), the change in size upon electrospinning and redispersion was 39%, that is, a S_f/S_i ratio of 1.4. As the NP size increased relative to the NF size (increasing NP:NF ratio), there was a decrease in the S_f/S_i ratio. Specifically, for the large NPs (NP:NF ratio 0.60), there was no significant change in NP size and a S_f/S_i ratio of 1.0 (Table 4).

These results indicate that matching the NP size to the NF size, that is, NP:NF ratio ~1, better maintains NP size upon redispersion compared to when the NP diameter is much smaller (less than half) than the NF diameter. When the NPs are small relative to the fiber diameter, multiple small particles in close proximity could aggregate as the liquid jet elongates and transitions to a solid fiber. In contrast, when the NP is similar in size to the resulting NF, the number of particles in the liquid jet as it transitions to a solid fiber is geometrically constrained to 1 particle. This geometric constraint may prevent NP-NP interactions that can lead to aggregation.

Table 3
Effect of NP Core Composition and Size on NP Size Stability After Reconstitution

NP Core	Initial NPs	Nanofiber	NP:NF	Reconstituted NPs	Change in	S_f/S_i
	Diameter (nm)	Diameter (nm)	Ratio	Diameter (nm)	Size (%)	
VE	118 ± 5	249 ± 32	0.47	159 ± 18	35	1.3
	144 ± 9	322 ± 56	0.45	169 ± 10	17	1.2
PS	112 ± 5	240 ± 32	0.47	189 ± 43	69	1.7
	192 ± 14	390 ± 37	0.49	223 ± 24	16	1.2

Table 4
Effect of NP:NF Ratio on NP Size Stability After Reconstitution

Initial NPs	Nanofiber	NP:NF	Reconstituted NPs	Change in	S_f/S_i
Diameter (nm)	Diameter (nm)	Ratio	Diameter (nm)	Size (%)	
95 ± 4	365 ± 36	0.26	133 ± 36	39	1.4
129 ± 2	326 ± 34	0.40	150 ± 18	16	1.2
174 ± 2	291 ± 37	0.60	174 ± 20	0	1.0

Notably, given the appropriate NP size relative to NF diameter ratio, drying NPs by blending and electrospinning with a water-soluble polymer is a promising approach that enables drying and redispersion with no significant change in NP size.

This observation related to NP:NF ratio is important for extending this approach to additional NP systems in future studies. Since NPs are often designed to be a certain size, varying NF size will be an important consideration. Fiber diameter of electrospun NFs is a complex function of electrospinning polymer properties, solvent, and process parameters.[50,51]

Practical Considerations

Building on these results, the NP loading in the polymer fibers was also examined. The loading of VE NPs (174 nm) was varied from 0.8 to 3.2 wt.% (mass of NP/mass of polymer). NP loading of 0.8 wt.% was the minimum NP concentration required to resolve the NP and PVA peaks using DLS. The final size was not significantly affected by the 4-fold increase in NP loading; the S_f/S_i ratios were 1.0 for the range of loadings examined (Supplementary Data, Table B). These loadings are comparable to drying FNP NPs via freeze drying[52] and spray freeze drying.[53]

Our focus has been on demonstrating that electrospinning is a viable approach to convert NPs to a dry form and that the NPs can be reconstituted to their original size. These preliminary results indicate that the reconstituted particle size is not significantly affected by the NP loading for the NP loadings examined. Further increasing the NP loading is of practical interest. Promising results maintaining NP size at high NPs using PVA excipients in spray freeze drying have been reported[31]; thus, higher loadings may be possible and will be addressed in future studies. Extension to electrospinnable polymers and biocompatible NP formulations that are U.S. Food and Drug Administration—approved for parenteral formulations will also be considered.[54-56]

Finally, preliminary experiments electrospinning NPs (VE core, PS-b-PEG stabilizer) with and without dialysis indicate that the presence of the organic solvent does not significantly affect fiber formation or NP reconstitution (Supplementary Data, Table D). In contrast, freeze drying (without excipient) after dialysis resulted in smaller redispersed particles when compared to nondialyzed samples.[23] Therefore, it may be possible to directly electrospin after FNP and avoid the purification step to remove the organic solvent. The presence of the organic solvent considering solvents other than THF, for example, dimethyl sulfoxide, during electrospinning will be further explored in future studies.

Conclusion

We demonstrate electrospinning as a new method to convert NP dispersions to a dry, stable form for long-term storage at room temperature. Using PEGylated NPs and PVA fibers as a model system, we show NPs can be stored at room temperature for at least 7 months and redispersed to their original size without sonication. Thus, encapsulating NPs in polymer fibers prevents changes in size due to Ostwald ripening. The dissolved polymer following electrospinning contributes negligibly to the osmolarity of the final NP dispersion.

The final NP size is affected by polymer fiber formation and NP properties. NP composition, NP size, and NF diameter relative to NP diameter are important considerations. Sizes of the NPs upon redispersion are maintained when the fiber diameter and NP diameter are comparable (NP:NF ratio ~1). NPs with liquid cores and larger particles better maintained their size when compared to NPs with solid cores and smaller particles, respectively. We attribute the observed differences to forces on the NPs during liquid jet-to-solid fiber transition during electrospinning.

Overall, electrospinning blends of NP dispersions and water-soluble, spinnable polymer is a novel approach for rapid, continuous drying of NPs at room temperature and redispersion to their original size at low osmolarity without sonication. This method overcomes the long-standing challenge of particle aggregation that occurs with traditional drying methods. Converting NP dispersions to dry, thermostable formulations will avoid the need for cold chain storage and enhance translation of nanomedicines to clinical practice.

Acknowledgments

The authors gratefully acknowledge Dr. Carlos Castano and the VCU Nano Characterization Center for their support and training, Dr. Hu Yang and Dr. Everett Carpenter for instrument access, and Dylan Rodene and Hajar Afilal for their assistance with experiments. This work was partially supported by startup funding at Virginia Commonwealth University, Virginia Commonwealth University Presidential Research Quest Fund, and NSF (Award number 1651957).

References

1. Gindy ME, Prud'homme RK. Multifunctional nanoparticles for imaging, delivery and targeting in cancer therapy. *Expert Opin Drug Deliv*. 2009;6(8):865-878.
2. Desai MP, Labhasetwar V, Walter E, Levy RJ, Amidon GL. The mechanism of uptake of biodegradable microparticles in Caco-2 cells is size dependent. *Pharm Res*. 1997;14(11):1568-1573.
3. Peer D, Karp JM, Hong S, Farokhzad OC, Margalit R, Langer R. Nanocarriers as an emerging platform for cancer therapy. *Nat Nanotechnol*. 2007;2(12):751-760.
4. Liu Y, Kathan K, Saad W, Prud'homme RK. Ostwald ripening of beta-carotene nanoparticles. *Phys Rev Lett*. 2007;98(3):036102.
5. Yusuf H, Nugraheni R, Mulyadi NA, Setyawan D, Rosita N. Phase behavior of dried—DDA liposomal formulation dispersed in HPMC matrix in the presence of saccharides. *Int J PharmTech Res*. 2017;10(1):50-56.
6. Figueroa CE, Adamson DH, Prud'homme RK. Effervescent redispersion of lyophilized polymeric nanoparticles. *Ther Deliv*. 2013;4(2):177-190.
7. D'Addio SM, Kafka C, Akbulut M, et al. Novel method for concentrating and drying polymeric nanoparticles: hydrogen bonding coacervate precipitation. *Mol Pharm*. 2010;7(2):557-564.
8. Franks F. Freeze-drying of bioproducts: putting principles into practice. *Eur J Pharm Biopharm*. 1998;45(3):221-229.
9. Freitas C, Müller RH. Spray-drying of solid lipid nanoparticles (SLN TM). *Eur J Pharm Biopharm*. 1998;46(2):145-151.
10. Iskandar F, Gradon L, Okuyama K. Control of the morphology of nanostructured particles prepared by the spray drying of a nanoparticle sol. *J Colloid Interface Sci*. 2003;265(2):296-303.
11. Anhorn MG, Mahler H-C, Langer K. Freeze drying of human serum albumin (HSA) nanoparticles with different excipients. *Int J Pharm*. 2008;363(1—2):162-169.
12. Cavalli R, Caputo O, Carlotti ME, Trotta M, Scarnecchia C, Gasco MR. Sterilization and freeze-drying of drug-free and drug-loaded solid lipid nanoparticles. *Int J Pharm*. 1997;148(1):47-54.
13. Schwarz C, Mehnert W. Freeze-drying of drug-free and drug-loaded solid lipid nanoparticles (SLN). *Int J Pharm*. 1997;157(2):171-179.
14. Abdelwahed W, Degobert G, Stainmesse S, Fessi H. Freeze-drying of nanoparticles: formulation, process and storage considerations. *Adv Drug Deliv Rev*. 2006;58(15):1688-1713.
15. Vehring R. Pharmaceutical particle engineering via spray drying. *Pharm Res*. 2008;25(5):999-1022.
16. Suzuki H, Hamao S, Seto Y, et al. New nano-matrix oral formulation of nano-precipitated cyclosporine A prepared with multi-inlet vortex mixer. *Int J Pharm*. 2017;516(1—2):116-119.
17. Jabłczyńska K, Janczewska M, Kulikowska A, Sosnowski TR. Preparation and characterization of biocompatible polymer particles as potential nanocarriers for inhalation therapy. *Int J Polym Sci*. 2015;2015:1-8.

18. Wanning S, Süverkrüp R, Lamprecht A. Pharmaceutical spray freeze drying. *Int J Pharm*. 2015;488(1):136-153.
19. Cheow WS, Ng MLL, Kho K, Hadinoto K. Spray-freeze-drying production of thermally sensitive polymeric nanoparticle aggregates for inhaled drug delivery: effect of freeze-drying adjuvants. *Int J Pharm*. 2011;404(1-2):289-300.
20. Tang C, Prud'homme RK. Targeted theragnostic nanoparticles via flash nanoprecipitation: principles of material selection. In: Vauthier C, Ponchel G, eds. *Polymer Nanoparticles for Nanomedicines*. Cham, Switzerland: Springer International Publishing; 2016:55-85.
21. Chacón M, Molpeceres J, Berges L, Guzmán M, Aberturas MR. Stability and freeze-drying of cyclosporine loaded poly(d,l lactide–glycolide) carriers. *Eur J Pharm Sci*. 1999;8(2):99-107.
22. Hinrichs WLJ, Manceñido FA, Sanders NN, et al. The choice of a suitable oligosaccharide to prevent aggregation of PEGylated nanoparticles during freeze thawing and freeze drying. *Int J Pharm*. 2006;311(1–2):237-244.
23. Figueroa CE. *Engineering Nanoparticles for Pharmaceutical Applications: Formulation and Freeze-Drying Techniques*. Ph.D. Dissertation. Princeton, NJ: Princeton University; 2014.
24. Abdelwahed W, Degobert G, Fessi H. A pilot study of freeze drying of poly(epsilon-caprolactone) nanocapsules stabilized by poly(vinyl alcohol): formulation and process optimization. *Int J Pharm*. 2006;309(1–2):178-188.
25. Saez A, Guzmán M, Molpeceres J, Aberturas MR. Freeze-drying of polycaprolactone and poly(d,l-lactic-glycolic) nanoparticles induce minor particle size changes affecting the oral pharmacokinetics of loaded drugs. *Eur J Pharm Biopharm*. 2000;50(3):379-387.
26. Burger C, Hsiao BS, Chu B. Nanofibrous materials and their applications. *Annu Rev Mater Res*. 2006;36(1):333-368.
27. Reneker DH, Chun I. Nanometre diameter fibres of polymer, produced by electrospinning. *Nanotechnology*. 1996;7(3):216-223.
28. Li D, Xia Y. Electrospinning of nanofibers: reinventing the wheel? *Adv Mater*. 2004;16(14):1151-1170.
29. Huang Z-M, Zhang Y-Z, Kotaki M, Ramakrishna S. A review on polymer nanofibers by electrospinning and their applications in nanocomposites. *Compos Sci Technol*. 2003;63(15):2223-2253.
30. Fridrikh SV, Yu JH, Brenner MP, Rutledge GC. Controlling the fiber diameter during electrospinning. *Phys Rev Lett*. 2003;90(14):144502.
31. Wang Y, Kho K, Cheow WS, Hadinoto K. A comparison between spray drying and spray freeze drying for dry powder inhaler formulation of drug-loaded lipid–polymer hybrid nanoparticles. *Int J Pharm*. 2012;424(1):98-106.
32. Sóti PL, Bocz K, Pataki H, et al. Comparison of spray drying, electroblowing and electrospinning for preparation of Eudragit E and itraconazole solid dispersions. *Int J Pharm*. 2015;494(1):23-30.
33. Torchilin VP. Multifunctional nanocarriers. *Adv Drug Deliv Rev*. 2012;64:302-315.
34. Bao G, Mitragotri S, Tong S. Multifunctional nanoparticles for drug delivery and molecular imaging. *Annu Rev Biomed Eng*. 2013;15(1):253-282.
35. Levine DH, Ghoroghchian PP, Freudenberg J, et al. Polymersomes: a new multi-functional tool for cancer diagnosis and therapy. *Methods*. 2008;46(1):25-32.
36. Tyrrell ZL, Shen Y, Radosz M. Fabrication of micellar nanoparticles for drug delivery through the self-assembly of block copolymers. *Prog Polym Sci*. 2010;35(9):1128-1143.
37. Tang C, Amin D, Messersmith PB, Anthony JE, Prud'homme RK. Polymer directed self-assembly of pH-responsive antioxidant nanoparticles. *Langmuir*. 2015;31(12):3612-3620.
38. Johnson BK, Prud'homme RK. Flash nanoprecipitation of organic actives and block copolymers using a confined impinging jets mixer. *Aust J Chem*. 2003;56(10):1021-1024.
39. Tang C, Saquing CD, Harding JR, Khan SA. In situ cross-linking of electrospun poly(vinyl alcohol) nanofibers. *Macromolecules*. 2010;43(2):630-637.
40. Dumas C, Meledandri CJ. Insights into the partitioning behavior of secondary surfactants in a microemulsion-based synthesis of metal nanoparticles: a DLS and 2D NMR spectroscopic investigation. *Langmuir*. 2015;31(26):7193-7203.
41. Mishael YG, Dubin PL. Toluene solubilization induces different Modes of mixed micelle growth. *Langmuir*. 2005;21(22):9803-9808.
42. (White paper). *Understanding the colloidal stability of protein therapeutics using dynamic light scattering*. Malvern, Worcestershire, UK: Malvern Instruments Limited; 2014.
43. Tang C, Ozcam AE, Stout B, Khan SA. Effect of pH on protein distribution in electrospun PVA/BSA composite nanofibers. *Biomacromolecules*. 2012;13(5):1269-1278.
44. Yu JH, Fridrikh SV, Rutledge GC. The role of elasticity in the formation of electrospun fibers. *Polymer*. 2006;47(13):4789-4797.
45. Rieger J. The glass transition temperature of polystyrene. *J Therm Anal Calorim*. 1996;46(3-4):965-972.
46. Yarin AL, Koombhongse S, Reneker DH. Bending instability in electrospinning of nanofibers. *J Appl Phys*. 2001;89(5):3018-3026.
47. Naraghi M, Arshad SN, Chasiotis I. Molecular orientation and mechanical property size effects in electrospun polyacrylonitrile nanofibers. *Polymer*. 2011;52(7):1612-1618.
48. Komrakova AE, Shardt O, Eskin D, Derksen JJ. Lattice Boltzmann simulations of drop deformation and breakup in shear flow. *Int J Multiph Flow*. 2014;59:24-43.
49. Ramanujan S, Pozrikidis C. Deformation of liquid capsules enclosed by elastic membranes in simple shear flow: large deformations and the effect of fluid viscosities. *J Fluid Mech*. 1998;361:117-143.
50. Tan S-H, Inai R, Kotaki M, Ramakrishna S. Systematic parameter study for ultra-fine fiber fabrication via electrospinning process. *Polymer*. 2005;46(16):6128-6134.
51. Ding B, Kim H-Y, Lee S-C, et al. Preparation and characterization of a nanoscale poly(vinyl alcohol) fiber aggregate produced by an electrospinning method. *J Polym Sci Part B Polym Phys*. 2002;40(13):1261-1268.
52. Chow SF, Wan KY, Cheng KK, et al. Development of highly stabilized curcumin nanoparticles by flash nanoprecipitation and lyophilization. *Eur J Pharm Biopharm*. 2015;94:436-449.
53. D'Addio SM, Chan JGY, Kwok PCL, Benson BR, Prud'homme RK, Chan H-K. Aerosol delivery of nanoparticles in uniform mannitol carriers formulated by ultrasonic spray freeze drying. *Pharm Res*. 2013;30(11):2891-2901.
54. Yu D-G, Shen X-X, Branford-White C, White K, Zhu L-M, Bligh SWA. Oral fast-dissolving drug delivery membranes prepared from electrospun polyvinylpyrrolidone ultrafine fibers. *Nanotechnology*. 2009;20(5):055104.
55. Mansour HM, Sohn M, Al-Ghananeem A, DeLuca PP. Materials for pharmaceutical dosage forms: molecular pharmaceutics and controlled release drug delivery aspects. *Int J Mol Sci*. 2010;11(9):3298-3322.
56. Wendorf J, Singh M, Chesko J, et al. A practical approach to the use of nanoparticles for vaccine delivery. *J Pharm Sci*. 2006;95(12):2738-2750.